Brain Tumor Pathology (2019) 36:169–173
https://doi.org/10.1007/s10014-019-00349-8

CASE REPORT

Anaplastic pleomorphic xanthoastrocytoma associated with an H3G34 mutation: a case report with review of literature

Shoh Sasaki[1,2] · Ran Tomomasa[3] · Sumihito Nobusawa[3] · Junko Hirato[3,4] · Tomoko Uchiyama[2] · Eishu Boku[5] · Toshiteru Miyasaka[6] · Takanori Hirose[7] · Chiho Ohbayashi[2]

Received: 12 July 2019 / Accepted: 23 July 2019 / Published online: 26 July 2019

Abstract

Here, we report a rare case of anaplastic pleomorphic xanthoastrocytoma (PXA) associated with an H3G34 mutation. A 12-year-old male presented with loss of appetite, vomiting, headache, and a generalized seizure, and CT revealed a 9.0 cm left frontal lobe mass with some septal walls and a localized high-density area suggestive of hemorrhage or calcification, causing severe midline shift. He emergently underwent subtotal resection and the tumor was morphologically diagnosed as anaplastic PXA. DNA sequencing identified an H3F3A G34R mutation and a TP53 R273H mutation, and immunohistochemically, ATRX nuclear expression was lost. In CNS tumors, H3G34 mutations are essentially detected in glioblastoma (GBM) or central nervous system primitive neuroectodermal tumors. Those tumors most likely comprise a single biological entity (high-grade glioma with H3G34 mutation) because of no significant difference in molecular profiling and prognosis between GBM and PNET morphologies. To our knowledge, our present case is the first one of anaplastic PXA associated with an H3G34 mutation, and whether it biologically corresponds to "high-grade glioma with H3G34 mutation" needs further studies.

Keywords Anaplastic pleomorphic xanthoastrocytoma · H3G34 mutation · Olig2 · ATRX · TP53

Introduction

Mutations in genes encoding histone 3 variants including *H3F3A*, *HIST1H3B*, and *HIST1H3C* have been identified in a subset of pediatric high-grade gliomas, and these mutations occur at two distinct residues, either K27 or G34 [1, 2]. Whereas the pathogenesis and clinicopathological features of H3K27M mutant tumors have been relatively well clarified, those of H3G34 mutant tumors not completely. CNS tumors with H3G34 mutations usually affect children and young adults and are typically located in the hemispheric region [3]. In CNS tumors, H3G34 mutations are essentially detected in glioblastoma (GBM) or central nervous system primitive neuroectodermal tumors (CNS-PNET) [4, 5]. Korshunov et al. demonstrated that there is no significant difference in molecular profiling and prognosis between GBM and PNET morphologies, suggesting that H3G34 mutant CNS tumors comprise a single biological entity (high-grade glioma with H3G34 mutation) [5]. Whereas a small portion of circumscribed/non-diffuse neuroepithelial tumors harbors H3K27M mutations [6], cases of such tumors harboring H3G34 mutations have not yet been reported in the well described literature as far as we know.

We herein report a rare case of anaplastic pleomorphic xanthoastrocytoma (PXA) associated with an H3G34 mutation.

✉ Shoh Sasaki
snowfairy18thankyou@yahoo.co.jp

1 Department of Pathology, Nara Prefecture General Medical Center, Nara, Japan

2 Department of Pathology, Nara Medical University Hospital, Nara, Japan

3 Department of Human Pathology, Gunma University Graduate School of Medicine, Gunma, Japan

4 Department of Pathology, Public Tomioka General Hospital, Gunma, Japan

5 Department of Neurosurgery, Nara Medical University Hospital, Nara, Japan

6 Department of Radiology, Nara Medical University Hospital, Nara, Japan

7 Department of Pathology, Hyogo Cancer Center, Hyogo, Japan

Case report

The patient was a 12-year-old male who presented with loss of appetite, vomiting, and headache. He visited psychiatric and pediatric clinics, and was diagnosed with acute stress disorder. He was referred to the Psychiatric Department of Nara Medical University Hospital for admission, and started antidepressant therapy. 1 week after admission, however, he presented with a generalized seizure. Non-contrast computed tomography (CT) of the head revealed a 9.0 cm left frontal lobe mass with some septal walls and a localized high-density area suggestive of hemorrhage or calcification, causing severe midline shift (Fig. 1a). He was referred to the Neurosurgical Department and emergently underwent subtotal resection (STR).

The histology was consistent with anaplastic pleomorphic xanthoastrocytoma (PXA) and an *H3F3A* G34R mutation was detected by DNA sequencing.

Contrast enhanced CT, which was taken a few days after first resection, revealed intensely enhancing lesions surrounding the postoperative resection cavity (Fig. 1b). He underwent second STR. Magnetic resonance imaging (MRI) of the head, which was taken 3 months after second resection, revealed enhancing multiple cystic lesions showing a tendency to an increase in the lesion size (Fig. 1c). He underwent third STR and started Temozolomide (TMZ) and radiation therapy. Despite beginning adjuvant treatment, MRI, which was taken 1 month after the third resection, revealed enhancing cystic lesions showing a tendency to an increase in the lesion size (Fig. 1d). He underwent the fourth STR and restarted TMZ and radiation therapy. Moreover, Bevacizumab (BV) was added to his regimen. MRI, which was taken 2 months after the fourth resection, revealed significant reduction of enhancing lesions compared to 2 weeks after the fourth resection (Fig. 1e). The histology of subsequent surgical specimens was similarly consistent with anaplastic PXA.

He was discharged from the hospital after completion of radiation therapy (60 Gy in 30 fractions). He is currently treated with single-agent BV as an outpatient. He is alive 1 year from the date of the first resection and MRI, which was taken 6 months after fourth resection, showed no evidence of an increase in the lesion size (Fig. 1f).

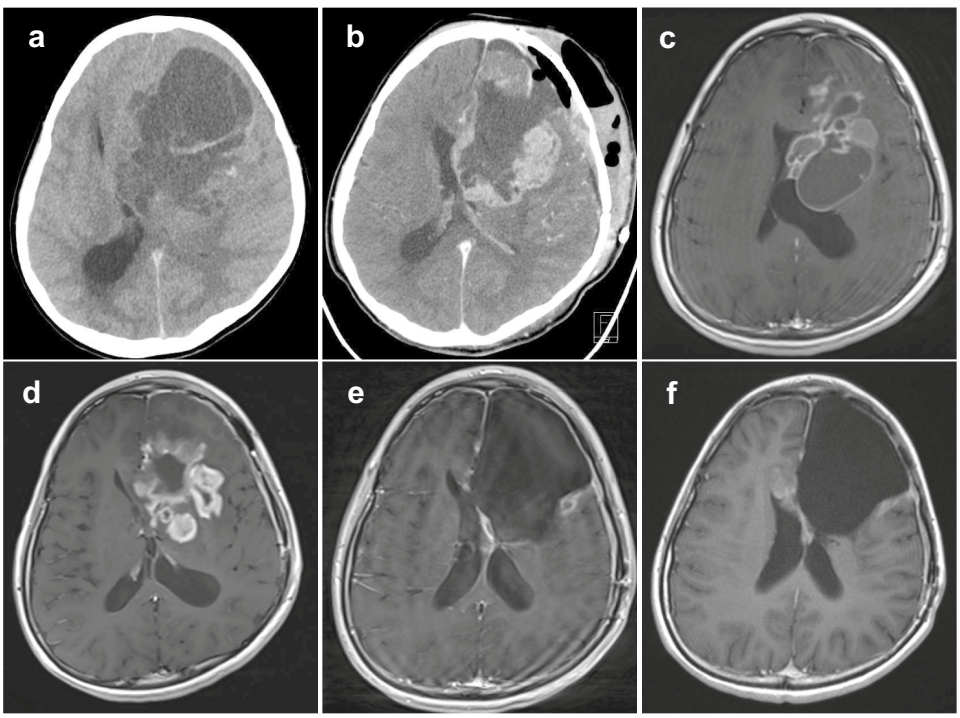

Fig. 1 Computed tomography (CT) and magnetic resonance imaging (MRI). **a** Preoperative CT shows a 9.0 cm left frontal lobe mass with some septal walls and a localized high-density area suggestive of hemorrhage or calcification, causing severe midline shift. **b** Contrast enhanced CT, which was taken a few days after first resection, shows intensely enhancing lesions surrounding the postoperative resection cavity. **c** T1-weighted image with gadolinium enhancement, which was taken 3 months after second resection, shows enhancing multiple cystic lesions. **d** T1-weighted image with gadolinium enhancement, which was taken 1 month after the third resection, shows enhancing irregular-shaped cystic lesions. **e** T1-weighted image with gadolinium enhancement, which was taken 2 months after fourth resection, shows significant reduction of enhancing lesions. **f** T1-weighted image with gadolinium enhancement, which was taken 6 months after fourth resection, shows no evidence of an increase in the lesion size

Pathologic findings

Histopathologic examination of all surgical specimens showed proliferation of pleomorphic mononucleated or multinucleated tumor cells with interstitial lymphocytes infiltration (Fig. 2a). In some areas, spindle tumor cells proliferated with fascicular arrangement (Fig. 2b). In other areas, small round tumor cells with a high N/C ratio infiltratively proliferated. Eosinophilic granular bodies and xanthomatous change were identified in spots (Fig. 2c, d). High mitotic activity (20 mitoses per 10 high-power fields) (Fig. 2e) and geographic necrosis were present. Microvascular proliferation was not detected. In some areas, individual tumor cells were surrounded by reticulin fibers (Fig. 2f).

Immunohistochemically, most tumor cells were positive for GFAP, nestin, and CD34 (Fig. 2g), and a small portion of tumor cells was positive for neurofilament protein (Fig. 2h). Tumor cells were immunonegative for Olig2 (Fig. 2i), IDH1R132H, and BRAF V600E. In addition, ATRX nuclear expression was lost (Fig. 2j) and overexpression of p53 was detected.

DNA sequencing revealed a *TP53* R273H mutation (Fig. 2k) and an *H3F3A* G34R mutation (Fig. 2l), while *IDH1/2*, *TERT* promoter, *BRAF* V600E, *H3F3A* K27M, *HIST1H3B*, and hot spot *FGFR1* (N546 and K656) mutations were not identified.

Discussion

We described a case of anaplastic PXA associated with an H3G34 mutation in a 12-year-old man. Based on the pathological findings such as proliferation of pleomorphic tumor cells, the presence of xanthomatous change, eosinophilic granular bodies, and reticulin fibers surrounding tumor cells, expression of CD34, and the presence of high mitotic activity and necrosis, the tumor was morphologically diagnosed as anaplastic PXA. Both *BRAF* V600E mutation and *CDKN2A/B* homozygous deletion commonly occur in PXA and anaplastic PXA [7–10]. Among gene alternations affecting the MAPK pathway other than *BRAF* mutations, *NF1* and *KRAS* mutations, and *NRF1-BRAF* and *ATG7-RAF1* fusions have been detected in PXA or anaplastic PXA [11, 12]. Although the *TP53* mutation was detected and ATRX

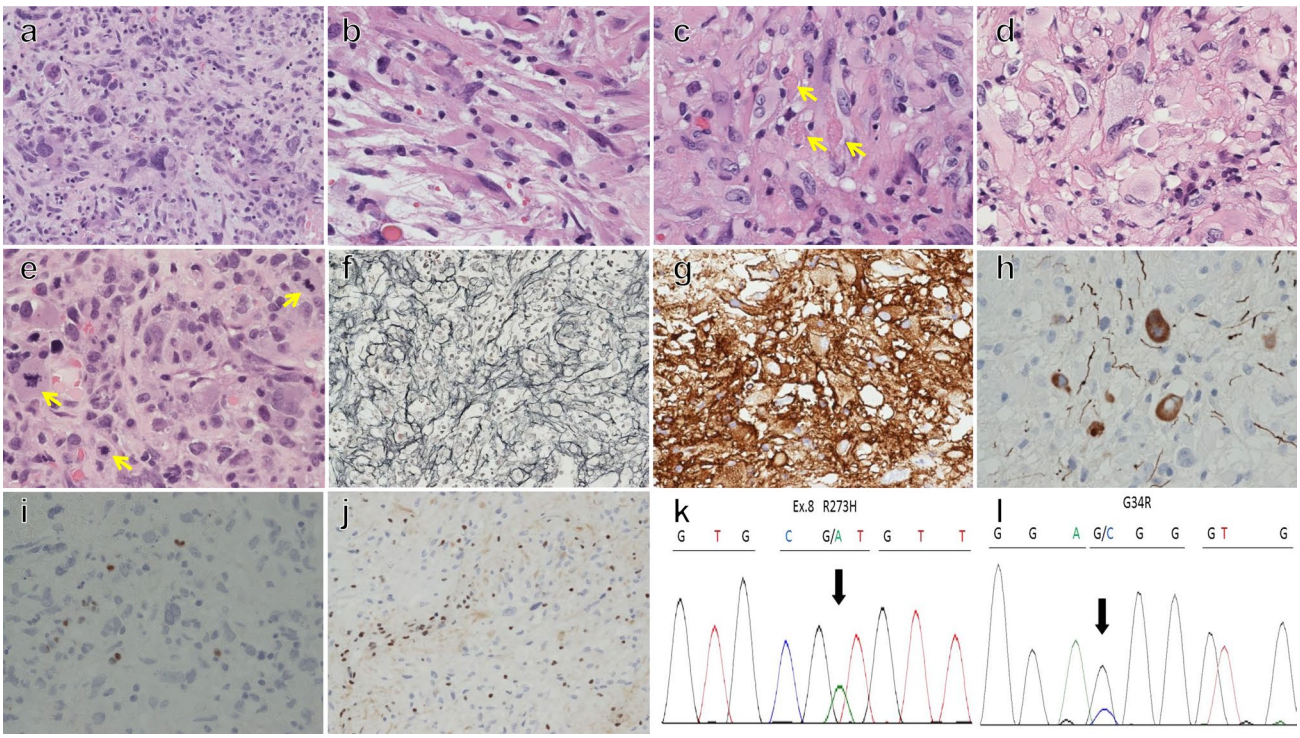

Fig. 2 Pathological findings. **a** Pleomorphic mononucleated or multinucleated tumor cells proliferate with interstitial lymphocytes infiltration. **b** Spindle tumor cells proliferate with fascicular arrangement. **c** Eosinophilic granular bodies are shown (arrow). **d** Tumor cells show xanthomatous change. **e** Three mitotic figures are shown in this figure (arrow). **f** Reticulin fibers surround individual tumor cells. **g** Tumor cells are immunopositive for CD34. **h** Small portion of tumor cells is immunopositive for neurofilament protein. **i**, **j** Tumor cells are immunonegative for **i** Olig2 and **j** ATRX, whereas non-neoplastic oligodendrocytes or vascular endothelial cells as internal control are immunopositive. **k**, **l** Sanger sequencing chromatogram shows presence of **k** a *TP53* R273H mutation and **l** an *H3F3A* G34R mutation in tumor cells

expression was lost in our case, these alternations uncommonly occur in PXA and anaplastic PXA [13, 14]. In addition, immunonegativity for Olig2 is unusual for PXA [11]. Probably, these findings reflect the presence of an H3G34 mutation.

In H3G34-mutated tumors, hypermethylation of OLIG1 and OLIG2 loci occurs, resulting in low levels of OLIG1 and OLIG2 gene expression [3]. In addition, the presence of H3F3A and ATRX mutations was strongly associated with alternative lengthening of telomeres and specific gene expression profiles, and H3G34 mutant tumors frequently harbor mutations in *TP53* and *ATRX* [1]. Thus, we finally made a diagnosis of anaplastic PXA associated with an H3G34 mutation.

Histones are critical factors which regulate almost all DNA metabolic processes, such as DNA replication, repair, and transcription. The definitive mechanisms underlying the pathogenesis and malignant transformation are different between H3K27M and H3G34 mutant tumors. The H3K27M mutation is located at the locus which is subject to post-translational modification. In addition, the H3K27M mutation prevents K27 methylation associated with polycomb-mediated gene repression, which causes reduction of global H3K27me3 levels and strikingly contributes to tumorigenesis [15, 16]. In contrast, H3G34 is not itself subject to post-translational modification, but it is in proximity to H3K36, whose methylation status is associated with active transcription, alternative splicing, dosage compensation, DNA replication, and DNA damage repair [17]. Although the specific roles contributing to tumorigenesis in H3G34-mutated tumors have not been clarified completely, some studies suggest several mechanisms underlying the pathogenesis and malignant transformation. Although nucleosomes harboring H3G34R/V mutations have no dominant effect on total cellular H3K36me2/me3 levels, they exhibit reduced H3K36me2/me3 levels on the same tail [18]. The structural change may prevent H3K36 from fitting the cavity of the SETD2 catalytic domain and other histone methyltransferases, resulting in the inhibition of H3K36 methylation [19]. Similarly, it may also prevent H3K36 from interacting with human mismatch recognition protein MutSα, leading to genome instability and tumorigenesis [19]. From the viewpoint of transcription factors, H3G34 mutations cause upregulation of MYCN through differential genomic binding of H3K36me3 [18].

With respect to treatment for PXA, extent of resection is the most important predictor of time to recurrence [20]. Although the role of adjuvant treatment for anaplastic PXA is not well established in the literature and management is highly controversial, some cases of anaplastic PXA with good response to chemotherapy and/or radiotherapy have been reported [21–23]. Marucci et al. examined MGMT promoter methylation status in 11 samples of PXA including two of anaplastic PXA [24]. In their study, only two cases of PXA were positive for MGMT promoter methylation and all of anaplastic PXA were negative, which raised doubts about the benefits of treating indistinctly aggressive PXA with TMZ. In vivo and vitro levels, some agents (e.g., TMZ, BV, and irinotecan) were effective against PXA [25, 26]. In our case, although it is difficult to understand the extent to which adjuvant treatment contributed to preventing tumor growth, we think that his prognosis is relatively better than expected by aggressive resection and adjuvant treatment.

Conclusion

We herein reported a rare case of anaplastic pleomorphic xanthoastrocytoma (PXA) associated with an H3G34 mutation. From the aspect of the biological significance of H3G34 mutations and therapeutic implications, it is interesting whether this tumor biologically corresponds to a single biological entity, so-called “high-grade glioma with H3G34 mutation”. Further studies are necessary to resolve this question.

References

1. Schwartzentruber J, Korshunov A, Liu XY et al (2012) Driver mutations in histone H3.3 and chromatin remodelling genes in paediatric glioblastoma. Nature 482(7384):226–231
2. Wu G, Broniscer A, McEachron TA et al (2012) Somatic histone H3 alterations in pediatric diffuse intrinsic pontine gliomas and non-brainstem glioblastomas. Nat Genet 44(3):251–253
3. Sturm D, Witt H, Hovestadt V et al (2012) Hotspot mutations in H3F3A and IDH1 define distinct epigenetic and biological subgroups of glioblastoma. Cancer Cell 22:425–437
4. Gessi M, Gielen GH, Hammes J et al (2013) H3.3 G34R mutations in pediatric primitive neuroectodermal tumors of central nervous system (CNS-PNET) and pediatric glioblastomas: possible diagnostic and therapeutic implications? J Neurooncol 112(1):67–72
5. Korshunov A, Capper D, Reuss D et al (2016) Histologically distinct neuroepithelial tumors with histone 3 G34 mutation are molecularly similar and comprise a single nosologic entity. Acta Neuropathol 131:137–146
6. Pratt D, Natarajan S, Banda A et al (2018) Circumscribed/non-diffuse histology confers a better prognosis in H3K27M-mutant gliomas. Acta Neuropathol 135(2):299–301
7. Dias-Santagata D, Lam Q, Vemovsky K et al (2011) BRAF V600E mutations are common in pleomorphic xanthoastrocytoma: diagnostic and therapeutic implications. PLoS One 6:e17948
8. Schindler G, Capper D, Meyer J et al (2011) Analysis of BRAF V600E mutation in 1320 nervous system tumors reveals high mutation frequencies in pleomorphic xanthoastrocytoma, ganglioglioma and extra-cerebellar pilocytic astrocytoma. Acta Neuropathol 121:397–405
9. Weber RG, Hoischen A, Ehrler M et al (2007) Frequent loss of chromosome 9, homozygous CDKN2A/p14(ARF)/CDKN2B deletion and low TSC1 mRNA expression in pleomorphic xanthoastrocytoma. Oncogene 26:1088–1097

10. Vaubel RA, Caron AA, Yamada S et al (2018) Recurrent copy number alterations in low-grade and anaplastic pleomorphic xanthoastrocytoma with and without BRAF V600E mutation. Brain Pathol 28:172–182
11. Zou H, Duan Y, Wei D et al (2019) Molecular features of pleomorphic xanthoastrocytoma. Hum Pathol 86:38–48
12. Phillips JJ, Gong H, Chen K et al (2016) Activating NRF1-BRAF and ATG7-RAF1 fusions in anaplastic pleomorphic xanthoastrocytoma without BRAF p. V600E mutation. Acta Neuropathol 132:757–760
13. Giannini C, Hebrink D, Scheithauer BW et al (2001) Analysis of p53 mutation and expression in pleomorphic xanthoastrocytoma. Neurogenetics 3(3):159–162
14. Murakami C, Yoshida Y, Yamazaki T et al (2019) Clinicopathological characteristics of circumscribed high-grade astrocytomas with an unusual combination of BRAF V600E, ATRX and CDKN2A/B alternations. Brain Tumor Pathol. https://doi.org/10.1007/s10014-019-00344-z
15. Simon JA, Kingston RE (2009) Mechanisms of Polycomb gene silencing: knowns and unknowns. Nat Rev Mol Cell Biol 10:697–708
16. Zhou VW, Goren A, Bernstein BE (2011) Charting histone modifications and the functional organization of mammalian genomes. Nat Rev Genet 12:7–18
17. Wagner EJ, Carpenter PB (2012) Understanding the language of Lys36 methylation at histone H3. Nat Rev Mol Cell Biol 13:115–126
18. Bjerke L, Mackay A, Nandhabalan M et al (2013) Histone H33 mutations drive pediatric glioblastoma through upregulation of MYCN. Cancer Discov 3(5):512–519
19. Fang J, Huang Y, Mao G et al (2018) Cancer-driving H3G34 V/R/D mutations block H3K36 methylation and H3K36me3-MutSα interaction. PNAS 115(38):9598–9603
20. Ida CM, Rodriguez FJ, Burger PC et al (2015) Pleomorphic xanthoastrocytoma: natural history and long-term follow-up. Brain Pathol 25(5):575–586
21. Chang HT, Latorre JG, Hahn S et al (2006) Pediatric cerebellar pleomorphic xanthoastrocytoma with anaplastic features: a case of long-term survival after multimodality therapy. Childs Nerv Syst 22:609–613
22. Okazaki T, Kageji T, Matsuzaki K et al (2009) Primary anaplastic pleomorphic xanthoastrocytoma with widespread neuroaxis dissemination at diagnosis—a pediatric case report and review of the literature. J Neurooncol 94:431–437
23. Alexiou GA, Moschovi M, Stefanaki K et al (2010) Malignant progression of a pleomorphic xanthoastrocytoma in a child. Neuropediatrics 41:69–71
24. Marucci G, Morandi L (2011) Assessment of MGMT promoter methylation status in pleomorphic xanthoastrocytoma. J Neurooncol 105:397–400
25. Bagriacik EU, Baykaner MK, Yaman M et al (2012) Establishment of a primary pleomorphic xanthoastrocytoma cell line: in vitro responsiveness to some chemotherapeutics. Neurosurgery 70:188–197
26. Thompson EM, Landi D, Ashley D et al (2018) Bevacizumab, irinotecan, temozolomide, tyrosine kinase inhibition, and MEK inhibition are effective against pleomorphic xanthoastrocytoma regardless of V600E status. J Neurooncol 140:261–268